HHS Public Access

Author manuscript

Anal Chem. Author manuscript; available in PMC 2019 June 27.

Published in final edited form as:

Anal Chem. 2018 June 19; 90(12): 7777–7783. doi:10.1021/acs.analchem.8b02042.

Development of an Electrochemical Paper-Based Analytical Device for Trace Detection of Virus Particles

Robert B. Channon[†,#], **Yuanyuan Yang**[†,#], **Kristen M. Feibelman**[‡], **Brian J. Geiss**[‡,‖], **David S. Dandy**[§,‖], and **Charles S. Henry**[*,†,§,‖]

[†] Department of Chemistry, Colorado State University, Fort Collins, Colorado 80523, United States

[‡] Department of Microbiology, Immunology, and Pathology, Colorado State University, Fort Collins, Colorado 80523, United States

[§] Department of Chemical and Biological Engineering, Colorado State University, Fort Collins, Colorado 80523, United States

[‖] School of Biomedical Engineering, Colorado State University, Fort Collins, Colorado 80523, United States

Abstract

Viral pathogens are a serious health threat around the world, particularly in resource limited settings, where current sensing approaches are often insufficient and slow, compounding the spread and burden of these pathogens. Here, we describe a label-free, point-of-care approach toward detection of virus particles, based on a microfluidic paper-based analytical device with integrated microwire Au electrodes. The device is initially characterized through capturing of streptavidin modified nanoparticles by biotin-modified microwires. An order of magnitude improvement in detection limits is achieved through use of a microfluidic device over a classical static paper-based device, due to enhanced mass transport and capturing of particles on the modified electrodes. Electrochemical impedance spectroscopy detection or West Nile virus particles was carried out using antibody runctionalized Au microwires, achieving a detection limit of 10.2 particles in 50 μL of cell culture media. No increase in signal is found on addition of an excess of a nonspecific target (Sindbis). This detection motif is significantly cheaper (~$1 per test) and faster (~30 min) than current methods, while achieving the desired selectivity and sensitivity. This sensing motif represents a general platform for trace detection of a wide range of biological pathogens.

Graphical Abstract

[*]**Corresponding Author** Chuck.Henry@colostate.edu.

[#]R.B.C. and Y.Y. contributed equally to this work.

ASSOCIATED CONTENT

Supporting Information

The Supporting Information is available free of charge on the ACS Publications website at DOI: 10.1021/acs.anal-chem.8b02042. Normalization of the EIS spectra, optimization of the EIS mediator concentration, investigations of Au-thiol stability, and analysis of SEM images (PDF)

The authors declare no competing financial interest.

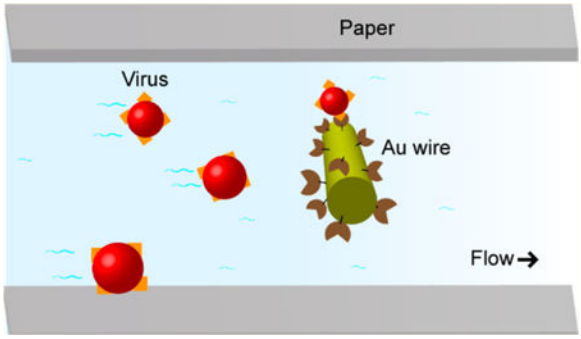

Viral pathogens cause millions of infections in the United States and abroad every year, resulting in severe morbidity and mortality in both the developing and developed world.[1,2] This problem is worsened by cocirculation of pathogens, for example, West Nile, chikungunya, Zika, and dengue viruses in Brazil. These diseases exhibit similar symptoms early in the infection making identification challenging.[3] To combat the spread of these viruses, sensitive detection techniques such as enzyme linked immunosorbent assay (ELISA) for IgM antibodies[4] and reverse transcriptase polymerase chain reaction (RT-PCR) for RNA[5] are employed. However, these methods require relatively long turnaround times (~days) in a centralized laboratory with professionally trained personnel at high expense. For example, it is estimated in Brazil that only 100 Zika virus samples a week can be processed through the existing infrastructure for the entire country.[6] This, coupled with the dramatic proliferation of emerging viruses, highlights the pressing need to develop inexpensive point-of-care (POC) technologies for rapid, sensitive, and accurate screening for patients suspected to have viral infections.[2] The ability to diagnose active infections on-site can improve patient compliance, allow physicians to tailor treatment options, and help prevent transmission of the pathogen.[2]

Common POC detection methods for viral targets include colorimetry,[7,8] fluorescence,[9,10] and lateral flow assays (LFAs).[11,12] Colorimetric approaches are simple and inexpensive but often suffer from poor sensitivities and detection limits[13] without additional amplification (loop-mediated isothermal amplification)[8] or detection (CRISPR - Clustered Regularly Interspaced Short Palindromic Repeats)[7] methods. Florescence detection is capable of excellent detection limits but can be expensive or require additional steps like immunomagnetic separation[9] or nucleic acid amplification,[10] increasing the complexity and assay time. LFAs are inexpensive, simple, and fast and have been used for POC detection of a range of viruses. Colorimetric detection is often used with LFAs, such that achieving the required detection limits can be challenging depending on the system,[14–16] and the transport of large particles in a single layer of paper is challenging.[17,18] In summary, there are no optimal POC diagnostics currently in use for viral pathogens.

Since their introduction in 2008, microfluidic paper-based analytical devices (μPADs) have been applied to a variety of fields, including environmental monitoring, disease diagnosis, and food quality control.[17,18] Through patterning of cellulosic paper, flow is self-generated and controlled via capillary action. μPADs have been coupled with several detection motifs including colorimetry, electrochemistry, and chemiluminescence, enabling fast analysis

through simple operation in POC environments. [17] Electrochemical PADs (ePADs) typically provide excellent sensitivity and good selectivity and are easily miniaturized.[17,19,20] ePADs have been previously employed for the sensing of biological targets including cancer biomarkers,[21] antibodies,[22] the influenza virus,[23] and neurotransmitters.[24]

Electrochemical impedance spectroscopy (EIS) is a particularly popular technique among electrochemical biosensors, as high sensitivities are commonplace, and the analyte of interest does not have to be electrochemically active.[25–30] EIS has been previously used for the sensitive detection of DNA, proteins, antibodies, viruses, and cells.[27,30–33] One drawback of EIS biosensors is their typical complexity and cost,[26] and achieving good specificity and sensitivity is a significant challenge for POC virus biosensors.[34] Given the high surface sensitivity of EIS, the electrode material, geometry, cleanliness, and modification strategy can all have significant effects on the sensitivity, specificity, and longevity of the sensor.[26,35] Au-monothiol coupling to generate a self-assembled monolayer is a particularly common coupling method for electrochemical biosensors, although the monolayer stability can vary depending on preparation and experimental conditions.[36] Alternate electrochemical approaches such as electrochemical-ap-tamer[37,38] and electrochemical-ELISA[22,39] have also been widely employed for the sensing of biological targets. One disadvantage of these approaches is that the capturing moiety must be modified with an electrochemical mediator (e.g., methylene blue) or catalyst (alkaline phosphatase)[22] adding further complexity to the sensor and potentially limiting the sensors longevity.

Herein, we describe an EIS ePAD platform capable of specifically detecting intact virus particles at clinically relevant concentrations in minutes. Simple patterning techniques are employed to create barriers on cellulosic paper, which can be coupled with functionalized Au microwire electrodes. Dithiol modification under strict conditions generates a robust base layer which can be cross-linked to antibodies through carbodiimide coupling. During detection, virus particles are captured onto the antibody-modified electrodes, resulting in a significant change in impedance. The proposed sensing platform and robust electrode modification strategy provides the groundwork for a broadly applicable chemistry to detect different intact viruses and other biological targets sensitively and specifically. Additionally, the inexpensive and generalized approach offers the potential for high-throughput manufacturing of disposable ePADs. This technology will ultimately allow multiplexed POC diagnostic detection of viral infection in a rapid and accurate manner.

EXPERIMENTAL SECTION

Chemicals and Materials.

30% hydrogen peroxide (H_2O_2), potassium nitrate (KNO_3), ethanolamine, amine-PEG2-biotin, 1-ethyl-3-(3-(dimethylamino)propyl)-carbodiimide HCl (EDC), and potassium ferricyanide ($Fe\text{-}(CN)_6^{3-}$) were purchased from Thermofisher Scientific (Fairlawn, NJ, USA). Anhydrous ethanol solution, 2-(*N*-morpholino)ethanesulfonic acid (MES) buffer, sulfo-*N*-hydroxsulfosuccinimide (NHS), lipoic acid, 11-mercaptoundecanoic acid (MUA), and potassium hexacyanoferrate(II) trihydrate ($Fe(CN)_6^{4-}$) were purchased from Sigma-Aldrich (St. Louis, MO). 6-(Ferrocenyl)hexanethiol ($Fc\text{-}(CH)_6SH$) was purchased from Santa Cruz Biotech (Dallas, TX). Sodium hydroxide (NaOH) was purchased from JT Baker (TX, USA).

All solutions were prepared in ultrapure Milli-Q water (18.2 MΩ cm, MilliPore, MA, USA). Whatman 1 chromatography paper was purchased from GE healthcare sciences (UK). Scotch Heavy Duty Shipping packing tape (3M) was purchased from Office Max. Streptavidin (SA) microparticles were purchased from Life Technologies. High purity silver paint was purchased from SPI Supplies (West Chester, PA). Au microwires (99.99% pure, 25 μm diameter) were purchased from California Fine Wire Company (Grover Beach, CA). 0.05 M pH 6.0 MES buffer was made with MES, and pH was adjusted to 6.0 with NaOH.

Device Fabrication.

Two device designs are tested within this study, namely a static-ePAD and a flow-ePAD as shown in Figures 4b and 4a, respectively. While the static-ePAD features a stationary microwell, the flow-ePAD utilizes a fan-shaped paper passive pump to generate fluid flow from the sample inlet. These device designs have been well characterized in previous works.[19,20] In short, Whatman 1 chromatography paper was patterned with wax using a Xerox ColorCube 8870 wax printer (Norwalk, CT) and then melted at 150 °C on a hot plate for 30 s to create hydrophobic barriers (circle for static-ePAD, fan shape for flow-ePAD). The backsides of both devices were sealed with packing tape to prevent leaking. For the static-ePAD, Au microwires were placed on the device and then held in place with laser cut packing tape (30 W Epilog Zing Laser Cutter and Engraver, Golden, CO). For the flow-ePAD, a second layer of Whatman 1 chromatography paper was laser cut to the dimensions of the wax printed microfluidic channels. The Au microwires were placed in between the two paper layers and the top of the device sealed with laser-cut packing tape, such that an inlet sample well is left uncovered for sample addition. For both devices, silver paint was used to make connections from the microwires to the potentiostat clips.

Electrode Modification.

Au microwires were modified with bioaffinity reagents to drive specific analyte binding through a stepwise bioconjugation process (Figure 1a). Twenty-five μm diameter Au microwires were cleaned by immersing in a NaOH solution containing 25% (v/v) H_2O_2 for 20 min. The clean Au microwires were then rinsed with DI water 3 times and then conditioned with anhydrous ethanol solution. To attach the carboxyl terminated alkane dithiol and generate a self-assembled monolayer, the freshly cleaned Au microwires were incubated in 1.0 mM lipoic acid in ethanol for 16 h in a N_2-infused aluminum foil-covered container, to achieve an O_2-free and UV-free environment.

After rinsing with DI water 3 times, the Au microwires were incubated in 0.05 M pH 6.0 MES buffer containing 200 μM amine-PEG2-biotin, 400 μM EDC, and 800 μM NHS for 4 h. After this carbondiimide cross-linking reaction, 0.10 M ethanolamine solution was added for 40 min to quench excess carboxyl groups on the Au surface. Furthermore, mixed self-assembled monolayers featuring a mix of capturing moieties and blocking groups are known to provide greater sensitivity due to reduced interunit screening.[30] The resulting Au microwires were carefully rinsed 3 times with DI water and dried under N_2 before assembly into the paper devices.

Electrochemical Impedance Spectroscopy.

All experiments were carried out using a CH660 potentiostat (CH Instruments, TX), using a home-built faraday cage at room temperature. Cyclic voltammetry and EIS measurements were carried out in a 2-electrode setup, with both electrodes modified with capturing groups to increase the sensitivity. This format (2-electrode setup with identical electrodes) is common for impedance biosensors.[29] Before EIS measurement in each device, cyclic voltammetry was carried out between –0.2 and 0.2 at 0.1 V s^{-1} in the $Fe(CN)_6^{3/4-}$ EIS mediator solution. This was found to equilibrate the surface resulting in more consistent EIS data. For EIS detection, an oscillation of ±10 mV about 0 V (vs Au) was applied at a frequency range of 100 kHz–0.05 Hz.

Virus Stocks and Controls.

West Nile virus (subtype Kunjin) was used to infect 70% confluent Baby Hamster Kidney 21 (BHK21) cells at an MOI of 0.1. The virus was incubated on cells for 72 h at 37 °C in Dulbecco's Modified Eagle Medium (ThermoFisher Scientific, Fairlawn, NJ, USA) supplemented with 10% fetal bovine serum and penicillin + streptomycin (cDMEM). Virus-containing media was harvested, centrifuged, and stored in single use aliquots at –80 °C. Viruses were titered by plaque assay as previously described.[40] For virus negative controls, media was harvested from uninfected BHK21 cells after 72 h, centrifuged, and stored at –80 °C. Standard curves were generated by diluting virus samples in a 1:10 dilution series in cDMEM.

RESULTS AND DISCUSSION

Device Characterization through Biotin Streptavidin Coupling.

As a proof of principle, biotin-terminated micro-wires were employed as recognition groups to bind with streptavidin modified (SA) microparticles ($K_d \approx 10^{-14}$ M), mimicking an antibody–antigen interaction. The electrode modification and capturing of the target analyte can be followed via cyclic voltammetry and EIS, as shown in Figures 1b and 1c, respectively. In this case, Au modification with thiol and biotin, followed by addition of 1×10^6 SA particles mL^{-1} (100 nm diameter), results in a clear increase in peak–peak separation (Figure 1b) as well as an increase in the resistance to charge transfer (R_{ct}, Figure 1c, diameter of semicircle), using a $Fe(CN)_6^{3/4-}$ redox couple. Similar electrode modification strategies have been demonstrated previously, for example with SS-DNA modified Au microwires and Au macroelectrodes for EIS detection of C-reactive protein[25] and *E. coli* single-strand binding protein,[41] respectively. To account for interdevice variabilities, the R_{ct} can be normalized via[42]

$$\%\Delta R_{ct} = 100 \times \frac{\left(R_{\text{ct after}} - R_{\text{ct before}}\right)}{R_{\text{ct before}}} \quad (1)$$

Assessment of the percentage increase in R_{ct}, before and after target analyte addition ($\%\Delta R_{ct}$), was found to give smaller interdevice variability compared to direct comparison of the final R_{ct} values after binding as described in the Supporting Information (Figure S1).

This is likely due to correction against device-to-device variations in fabrication and electrode modification, as previously discussed by Gupta et al.[42] Use of a 2-electrode setup with both wires modified identically was found to improve the assay sensitivity (data not shown), likely due to increased surface capturing sites. $Fe(CN)_6^{3/4-}$ (10 mM) was employed as a EIS mediator, with the high concentration minimizing R_{ct}, making changes on binding more significant (Figure S2).

Stability of Au-Thiol Self-Assembled Monolayers.

Coupling of thiols to Au to generate a self-assembled monolayer is a common electrode modification strategy due to the reaction's spontaneous and mild conditions. Despite widespread use in many biological applications,[25] thiol instability, especially in the presence of $Fe(CN)_6^{3/4-}$, is a poorly understood issue, resulting in unstable modifications and erroneous results.[36] Several approaches to increase the thiol-Au SAM stability have been investigated including UV and O_2 free environments and the use of multidentate instead of monodentate thiols.[36,43]

The stability of thiol modified Au microwires was first investigated through binding of a ferrocene terminated monothiol (Fc-$(CH)_6$SH) under different experimental conditions, as described in the Supporting Information (S2). Cyclic voltammetry of the modified electrodes, after different storage conditions between modification and fabrication into static-ePADs, demonstrated that storage in a N_2-infused and dark environment provided significant enhancements in the monolayer stability (Figure S3). This is in line with previous investigations of thiol-gold self-assembled monolayer stabilities.[36] Next, MUA (a monodentate thiol) was contrasted with lipoic acid (dithiol) to investigate the self-assembled monolayer stability. Au wires were modified with either mono- or dithiol carboxylic acid, followed by biotin (Figure 1a) for the capturing of SA microbeads in a static-ePAD. The dithiol was found to give a greater sensitivity (17.5 vs 11.7) and smaller errors in $\%\Delta R_{ct}$ compared to the capturing of SA microbeads with the monodentate thiol, as shown in Figure 2. This difference is likely due to the instability of the monothiol modification, resulting in a reduction of self-assembled monolayer density and larger variance. The device longevity was tested through capturing of 1.0×10^6 SA particles mL^{-1} from 1–14 days after device fabrication, as described in the Supporting Information (S2, Figure S4). A 68% increase in signal ($\%\Delta R_{ct}$) was observed over the first 3 days, followed by a plateau in signal indicating a stable surface over the 15 days investigated.

Flow vs Static Paper-Based Devices.—To characterize the system, SA particles ranging in size from 40 nm to 56 μm diameter were added to static-ePADs, as shown in Figure 3. The SA particles were prepared in 0.10 M NaCl buffer, and 10 mM $Fe(CN)_6^{3/4-}$ was prepared in 0.10 M KNO_3 as an electrochemical mediator. Sensing was carried out through addition of 50 μL of $Fe(CN)_6^{3/4-}$, followed by 50 μL of SA solution, and then 50 μL of $Fe(CN)_6^{3/4-}$ again. For the static-ePAD, the SA particles were left on the device for 10 min. For the flow-ePAD, injections were added and allowed to flow until depletion of the inlet (~10 min), and EIS was carried out after $Fe(CN)_6^{3/4-}$ had reached the electrodes. A roughly linear increase in $\%\Delta R_{ct}$ was observed on capture of increasing diameter particles (Figure 3 inset, $R^2 = 0.9866$), consistent with greater steric blocking of $Fe(CN)_6^{3/4-}$

diffusion about the microwire surface. Therefore, the proposed method is amenable to a wide size range of target species, from small viruses to intact cells.

The static-ePAD and flow-ePAD platforms were compared for trace detection of 100 nm diameter SA particles (Figure 4). Similar sensitivities (17.4 vs 17.5 ΔR_{ct} particles^{-1} mL), but a wider linear range (2.0×10^2 to 2.0×10^{10} vs 2.0×10^4 to 2.0×10^{10} particles mL^{-1}) and lower detection limit (7.4×10^3 vs 8.4×10^4 particles mL^{-1}), were observed for flow-ePADs compared to static-ePADs. The modified Au microwires were placed between two paper layers in the flow-ePADs, such that the sample added to the inlet flows down along the channel (~25 μm gap between paper layers, channel width = 1.8 mm) toward the fan-shaped passive pump, which drives the fluid flow via capillary action (Figure 4a).[20] Thus, we hypothesize the lower detection limits in flow-ePADs are due to increased mass transport of species to the electrode surface, via convection and diffusion. Conversely, the static-ePAD (Figure 4b) relies solely on diffusive transport of the target analyte to the electrode surface. Moreover, the closed nature of the flow-ePADs (sealed with packing tape) makes handling and disposal simpler compared to the open static-ePAD.

The binding was further characterized through scanning electron microscopy (SEM) on biotin-modified electrodes before (Figure 5a) and after (Figure 5b) addition of 1.0×10^6 SA particles mL^{-1}. The SEM images were then analyzed to establish the density of bound beads through a circle-finding script in MATLAB, as described in the Supporting Information (S3). After modification in a static-ePAD for 10 min, the density was found to be 2.8×10^4 SA particles mm^{-2} (averaged between 5 images across the electrode surface). This corresponds to ~7,600 bound particles across the two microwires, an active capturing group separation of ~6.0 μm, a surface coverage of 0.09%, and a capturing efficiency of ~0.76% of the total SA particles. These values are reasonable based on literature values for modified Au electrodes.[44] Diffusion coefficients (D) of viruses and micrometer particles are typically around 5.0×10^{-8} cm^2 s^{-1} and dependent on the virus/particle size.[45] Thus, assuming mass-transport limited capturing (fast binding kinetics compared to diffusion), during a 10 min deposition time (t), particles will diffuse an average distance (x) of 78 μm based on

$$x = \sqrt{2Dt} \quad (2)$$

Thus, ~0.82% of the 50 μL aliquot volume (~0.41 μL) is sampled between the two microwires, and the effective capturing efficiency in the static-ePADs is ~93% of the aliquot. Multilayer μPADs (featuring two layers of paper) have been shown to increase mass transport and facilitate greater sampling of the aliquot compared to static measurements.[46] Therefore, these data corroborate the lower detection limits in the flow-ePAD format over the static-ePAD format.

Trace Detection of West Nile Virus.—To demonstrate the method scope, flow-ePADs were applied for detection of West Nile virus particles (WNV, subtype Kunjin). WNV is an arthropod-borne flavivirus typically transmitted to humans by female Culex species mosquitos.[1] Infection with WNV can lead to severe neurological symptoms such as meningitis or encephalitis, and there are currently no available vaccines or therapeutic

treatments for humans.[1,47] Between 1999 and 2013 there were 17,463 verified cases of WNV infection in the US, and current studies predict increasing rates of WNV transmission as global temperatures increase and create climatic conditions favorable to mosquito vectors.[48,49] Common approaches such as antibody capture ELISA or RT-PCR are difficult to carry out in resource limited settings.[2] Therefore, POC techniques are needed for increased surveillance of WNV spread in patients and vector species to divert virus control efforts to those areas with the greatest need.

Using a similar modification procedure to the one shown in Figure 1a, Au microwires were modified with lipoic acid, followed by a flavivirus-envelope protein specific 4G2 antibody (20 μg mL^{-1})[50] through EDC/NHS coupling, before assembly into flow-ePADs. After thawing, West Nile and Sindbis viruses were serially diluted with cell culture media to their required concentrations and then kept on ice during aliquot extraction for measurement. The average viral titer was ~1 h between different devices/measurements. As shown in Figure 6, an antibody concentration of 20 μg/mL was found to give a significant increase in $\%\Delta R_{ct}$ for addition of 1×10^6 WNV particles mL^{-1} (blue circles) compared to a control of viral media (red squares). Note the concentratsion tested are in line with literature values for virus sensors.[50] At lower antibody concentrations, similar $\%\Delta R_{ct}$ were observed for both target and control tests due to low modification densities. For example, note that the 2 μg/mL in Figure 6 has the control mean data point at a higher $\%\Delta R_{ct}$ than the WNV target. Although not quite statistically significant (unpaired t-test $p = 0.096$), this erroneous result may be an artifact of the small sample size ($n = 3$).

To assess the assay sensitivity and capacity for trace detection of virus particles, 50 μL of 1.0×10^3–1.0×10^6 WNV particles mL^{-1} in cell culture media were added, generating a linear response as shown in Figure 7 (triangles, $n = 4$). A nonspecific test was carried out using an excess of nonrelated Sindbis virus particles[51] (1.0×10^7 particles mL^{-1}, green circle, $n = 4$), finding a low $\%\Delta R_{ct}$ (244% ± 24). A limit of detection of 2.0×10^3 WNV particles mL^{-1} or 10.2 WNV particles within the 50 μL aliquot was found (Sindbis $\%\Delta R_{ct}$ + 3 × standard error of the mean/slope), which is similar to that achievable by RT- PCR, ELISA, or other literature approaches.[4,5,34] Note, the nonspecific value is used in place of a blank as it is more representative of a real system, as previously discussed.[26] Also, the error bars in Figure 7 represent the standard error of the mean ($n = 4$). Further, these data also correspond to Figure S1 in the Supporting Information, highlighting the need for normalization of the EIS signals. No statistically significant correlation was observed between measurement number and signal, indicating the electrodes and antibodies were stable over the experimental time (~1 h between fabrication and measurement, unpaired t-test $p = 0.311$). Our detection limits are below the clinical range for WNV, which varies between 1×10^2 and 1×10^6 genomic equivalents per mL, depending on the location (tissue in the body), matrix (blood or urine), and stage of infection.[52,53]

CONCLUSIONS

A sensitive, specific, inexpensive, and fast flow-ePAD sensor for virus particles has been developed. This approach is ideally suited to sensing in resource limited settings, given EIS-based sensing motifs are easily miniaturized and controllable via a smartphone.[54] Use of

dithiol-Au and carbodiimide coupling is shown to provide a stable electrode with a high density (2.8×10^4 SA particles mm^{-2}) of capturing groups (e.g., antibodies). The sensing motif has broad applicability to a range of biological targets for POC detection, particularly for monitoring transmission of other closely related flavivirus species such as yellow fever and Zika viruses in areas where access to traditional methods of disease diagnosis and monitoring are limited. Given the small size of WNV particles (~50 nm diameter),[55] we anticipate similar or better detection limits for other similar or larger size targets, allowing for variance in binding kinetics between different target-capture systems. Future work will seek to apply this sensing motif to different biological targets and reduce the assay time through optimization of the device geometry to compete with the speed of LFAs (~10 min).[46]

Supplementary Material

Refer to Web version on PubMed Central for supplementary material.

ACKNOWLEDGMENTS

R.B.C., Y.Y., and C.S.H. thank CSU through the Catalyst for Innovative Partnerships program and the USDA through the National Wildlife Research Center (NWRC, AP17WSNWRC00C027) for project support. K.M.F. and B.J.G. are grateful for partial support from NIH/NIAID R01 AI114675. R.B.C. is grateful for partial support from NIOSH R01 OH010662.

REFERENCES

(1). Mackenzie JS; Gubler DJ; Petersen LR Nat. Med. 2004, 10, S98. [PubMed: 15577938]

(2). Peeling RW; Mabey D Clin. Microbiol. Infect. 2010, 16, 1062–1069. [PubMed: 20670288]

(3). Keasey SL; Pugh CL; Jensen SM; Smith JL; Hontz RD; Durbin AP; Dudley DM; O'Connor DH; Ulrich RG Clin. Vaccine Immunol. 2017, 24, e00036–17.

(4). Galula JU; Chang G-JJ; Chuang S-T; Chao D-YJ Clin. Microbiol. 2016, 54, 412–422.

(5). Fall G; Faye M; Weidmann M; Kaiser M; Dupressoir A; Ndiaye EH; Ba Y; Diallo M; Faye O; Sall AA Vector Borne Zoonotic Dis. 2016, 16, 781–789. [PubMed: 27710313]

(6). Samarasekera U; Triunfol M Lancet 2016, 387, 521–524. [PubMed: 26852261]

(7). Pardee K; Green AA; Takahashi MK; Braff D; Lambert G; Lee JW; Ferrante T; Ma D; Donghia N; Fan M; Daringer NM; Bosch I; Dudley DM; O'Connor DH; Gehrke L; Collins JJ Cell 2016, 165, 1255–1266. [PubMed: 27160350]

(8). Song J; Mauk MG; Hackett BA; Cherry S; Bau HH; Liu C Anal. Chem. 2016, 88, 7289–7294. [PubMed: 27306491]

(9). Zhao W; Zhang W-P; Zhang Z-L; He R-L; Lin Y; Xie M; Wang H-Z; Pang D-W Anal. Chem. 2012, 84, 2358–2365. [PubMed: 22309154]

(10). Wu S-JL; Lee EM; Putvatana R; Shurtliff RN; Porter KR; Suharyono W; Watts DM; King C-C; Murphy GS; Hayes CG; Romano JW J. Clin. Microbiol. 2001, 39, 2794–2798. [PubMed: 11473994]

(11). Burkhalter KL; Horiuchi K; Biggerstaff BJ; Savage HM; Nasci RS J. Am. Mosq. Control Assoc. 2014, 30, 21–30. [PubMed: 24772673]

(12). Ryan J; Dave K; Emmerich E; Fernandez B; Turell M; Johnson J; Gottfried K; Burkhalter K; Kerst A; Hunt A; Wirtz R; Nasci RJ Med. Entomol. 2003, 40, 95–99.

(13). Herrmann S; Leshem B; Landes S; Rager-Zisman B; Marks R S. Talanta 2005, 66, 6–14.

(14). Le TT; Chang P; Benton DJ; McCauley JW; Iqbal M; Cass AE G. Anal. Chem. 2017, 89, 6781–6786.

(15). Zhu M; Zhang W-n.; Tian J.-y.; Zhao W.-y.; Chen Z.-q.; Sun L.-h.; Xue F; Liu Y; Tan X.-q.; Wang L.-m.; Liu F.-q.; Tao X.- r. J. Virol. Methods 2016, 235, 51–57. [PubMed: 27235541]

(16). Tang R; Yang H; Gong Y; Liu Z; Li X; Wen T; Qu Z; Zhang S; Mei Q; Xu F Sci. Rep. 2017, 7, 1360. [PubMed: 28465588]

(17). Yang Y; Noviana E; Nguyen MP; Geiss BJ; Dandy DS; Henry CS Anal. Chem. 2017, 89, 71–91. [PubMed: 27936612]

(18). Gong MM; Sinton D Chem. Rev. 2017, 117, 8447–8480. [PubMed: 28627178]

(19). Adkins JA; Henry CS Anal. Chim. Acta 2015, 891, 247–254. [PubMed: 26388383]

(20). Adkins JA; Noviana E; Henry CS Anal. Chem. 2016, 88, 10639–10647. [PubMed: 27749031]

(21). Ma C; Li W; Kong Q; Yang H; Bian Z; Song X; Yu J; Yan M Biosens. Bioelectron. 2015, 63, 7–13. [PubMed: 25048447]

(22). Glavan AC; Christodouleas DC; Mosadegh B; Yu HD; Smith BS; Lessing J; Fernandez-Abedul MT; Whitesides GM Anal. Chem. 2014, 86, 11999–12007. [PubMed: 25470031]

(23). Devarakonda S; Singh R; Bhardwaj J; Jang J Sensors 2017, 17, 2597.

(24). Feng Q-M; Cai M; Shi C-G; Bao N; Gu H-Y Sens. Actuators, B 2015, 209, 870–876.

(25). Songjaroen T; Feeny RM; Mensack MM; Laiwattanapaisal W; Henry CS Sens. Bio-Sens. Res. 2016, 8, 14–19.

(26). Daniels JS; Pourmand N Electroanalysis 2007, 19, 1239–1257. [PubMed: 18176631]

(27). Bogomolova A; Komarova E; Reber K; Gerasimov T; Yavuz O; Bhatt S; Aldissi M Anal. Chem. 2009, 81, 3944–3949. [PubMed: 19364089]

(28). Chang B-Y; Park S-M Annu. Rev. Anal. Chem. 2010, 3, 207–229.

(29). Lasia A Electrochemical impedance spectroscopy and its applications; Springer: 2014; DOI: 10.1007/0-306-46916-2_2.

(30). Katz E; Willner I Electroanalysis 2003, 15, 913–947.

(31). Li Z; Fu Y; Liao M; Li Y Anal. Methods 2017, 9, 5238–5248.

(32). Yu C; Wang Q; Li W; Li Y; Liu S; Bao N; Gu H Nanotechnology 2015, 26, 325501. [PubMed: 26201357]

(33). Palomar Q; Gondran C; Holzinger M; Marks R; Cosnier S Biosens. Bioelectron. 2017, 97, 177–183. [PubMed: 28599177]

(34). Foord AJ; Boyd V; White JR; Williams DT; Colling A; Heine HG J. Virol. Methods 2014, 203, 65–72. [PubMed: 24690622]

(35). Putzbach W; Ronkainen N Sensors 2013, 13, 4811. [PubMed: 23580051]

(36). Srisombat L; Jamison AC; Lee T R Colloids Surf. A 2011, 390, 1–19.

(37). Schoukroun-Barnes LR; Macazo FC; Gutierrez B; Lottermoser J; Liu J; White RJ. Annu. Rev. Anal. Chem. 2016, 9, 163–181.

(38). Plaxco KW; Soh HT Trends Biotechnol 2011, 29, 1–5. [PubMed: 21106266]

(39). Safaei TS; Mohamadi RM; Sargent EH; Kelley SO ACS Appl. Mater. Interfaces 2015, 7, 14165–14169. [PubMed: 25938818]

(40). Otte K; Steinbruchel D; Kain H; Kemp E In Transplantation proceedings; Elsevier: 1992; pp 449–450.

(41). Ricci F; Bonham AJ; Mason AC; Reich NO; Plaxco KW Anal. Chem. 2009, 81, 1608–1614. [PubMed: 19199570]

(42). Gupta RK; Periyakaruppan A; Meyyappan M; Koehne JE Biosens. Bioelectron. 2014, 59, 112–119. [PubMed: 24709327]

(43). Lazar J; Schnelting C; Slavcheva E; Schnakenberg U Anal. Chem. 2016, 88, 682–687. [PubMed: 26618671]

(44). White RJ; Phares N; Lubin AA; Xiao Y; Plaxco KW Langmuir 2008, 24, 10513–10518. [PubMed: 18690727]

(45). Harvey JD Virology 1973, 56, 365–368. [PubMed: 4355532]

(46). Channon RB; Nguyen M; Scorzelli A; Henry E; Volckens J; Dandy D; Henry C Lab Chip 2018, 18, 793–802. [PubMed: 29431751]

(47). Sejvar J Viruses 2014, 6, 606. [PubMed: 24509812]

(48). Fros JJ; Geertsema C; Vogels CB; Roosjen PP; Failloux A-B; Vlak JM; Koenraadt CJ; Takken W; Pijlman GP PLoS Neglected Trop. Dis. 2015, 9, e0003956.

(49). Vogels CBF; Hartemink N; Koenraadt CJ M. Sci. Rep. 2017, 7, 5022.

(50). Henchal EA; Gentry MK; McCown JM; Brandt WE Am. J. Trop. Med. Hyg. 1982, 31, 830–836. [PubMed: 6285749]

(51). Adelman Z; Blair C; Carlson J; Beaty B; Olson K Insect Mol. Biol. 2001, 10, 265–273. [PubMed: 11437918]

(52). Barzon L; Pacenti M; Franchin E; Pagni S; Martello T; Cattai M; Cusinato R; Palu GJ Infect. Dis. 2013, 208, 1086–1092.

(53). Kelley SO ACS Sens. 2017, 2, 193–197. [PubMed: 28723142]

(54). Jiang J; Wang X; Chao R; Ren Y; Hu C; Xu Z; Liu GL Sens. Actuators, B 2014, 193, 653–659.

(55). Kramer LD; Li J; Shi P-Y Lancet Neurol. 2007, 6, 171–181. [PubMed: 17239804]

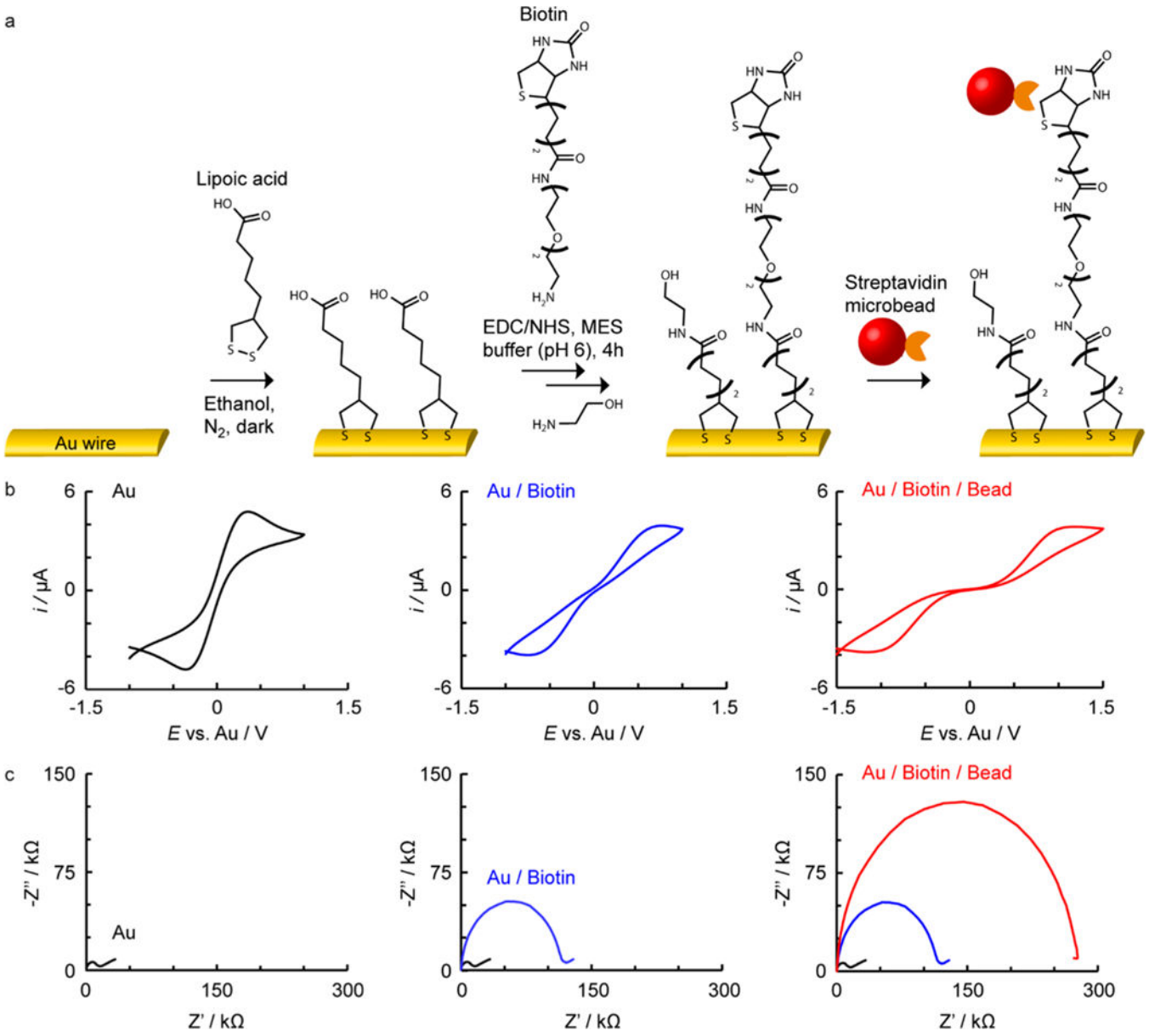

Figure 1.

a) Reaction scheme with b) representative corresponding cyclic voltammograms and c) EIS for Au microwire electrodes at different stages of modification with biotin, for capture of SA particles on a static-ePAD.

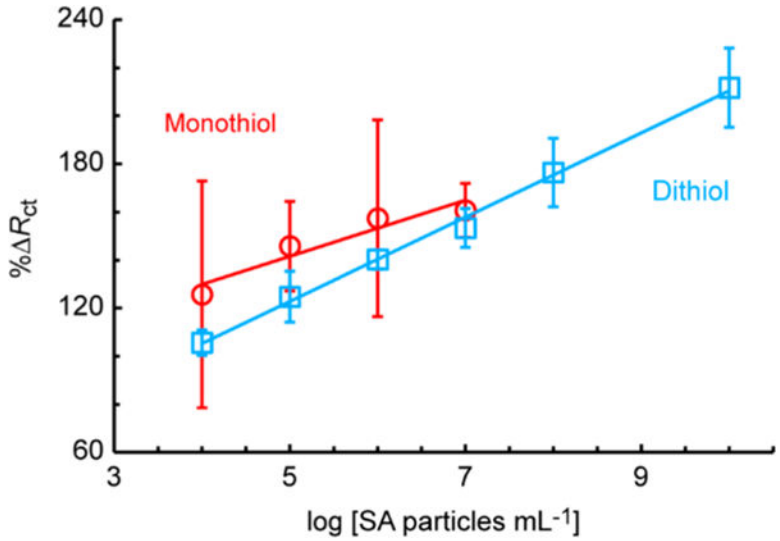

Figure 2.

Comparison of monothiol (11-mercaptoundecanoic acid) vs dithiol (lipoic acid) modification of Au microwires, for detection of 100 nm SA particles in static-ePADs, $n = 4$, sensitivity = 11.7 and 17.5 particles^{-1} mL, and $R^2 = 0.9062$ and 0.9963 for the mono- and dithiol, respectively.

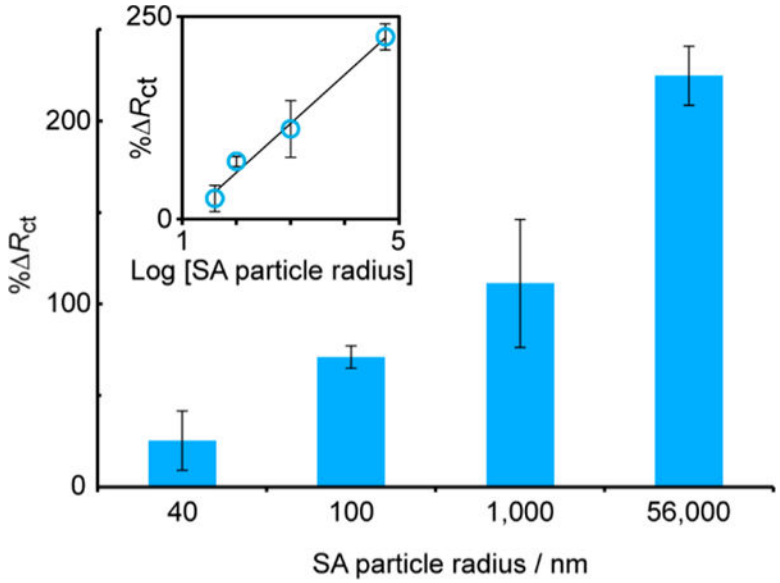

Figure 3.

Effect of SA particle size on $\%\Delta R_{ct}$ for 1×10^6 SA particles mL^{-1} captured on biotin-modified microwires in a static-ePAD, $R^2 = 0.9866$, $n = 4$.

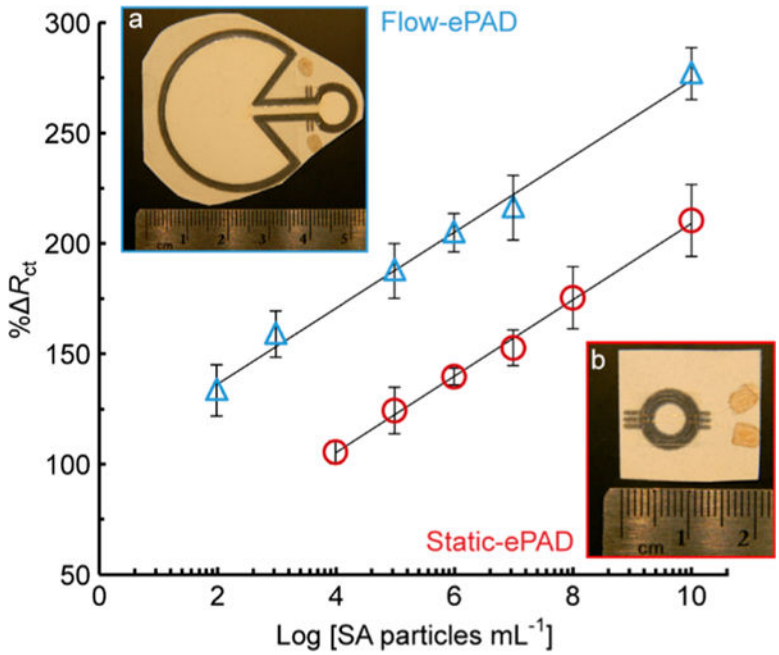

Figure 4.

Calibration curve for flow-ePADs (blue triangles, a inset, R^2 = 0.9932) and static-ePADs (red circles, b inset, R^2 = 0.9963) for detection of different concentrations of 100 nm diameter SA particles, 50 μL aliquot in phosphate buffer, n = 4.

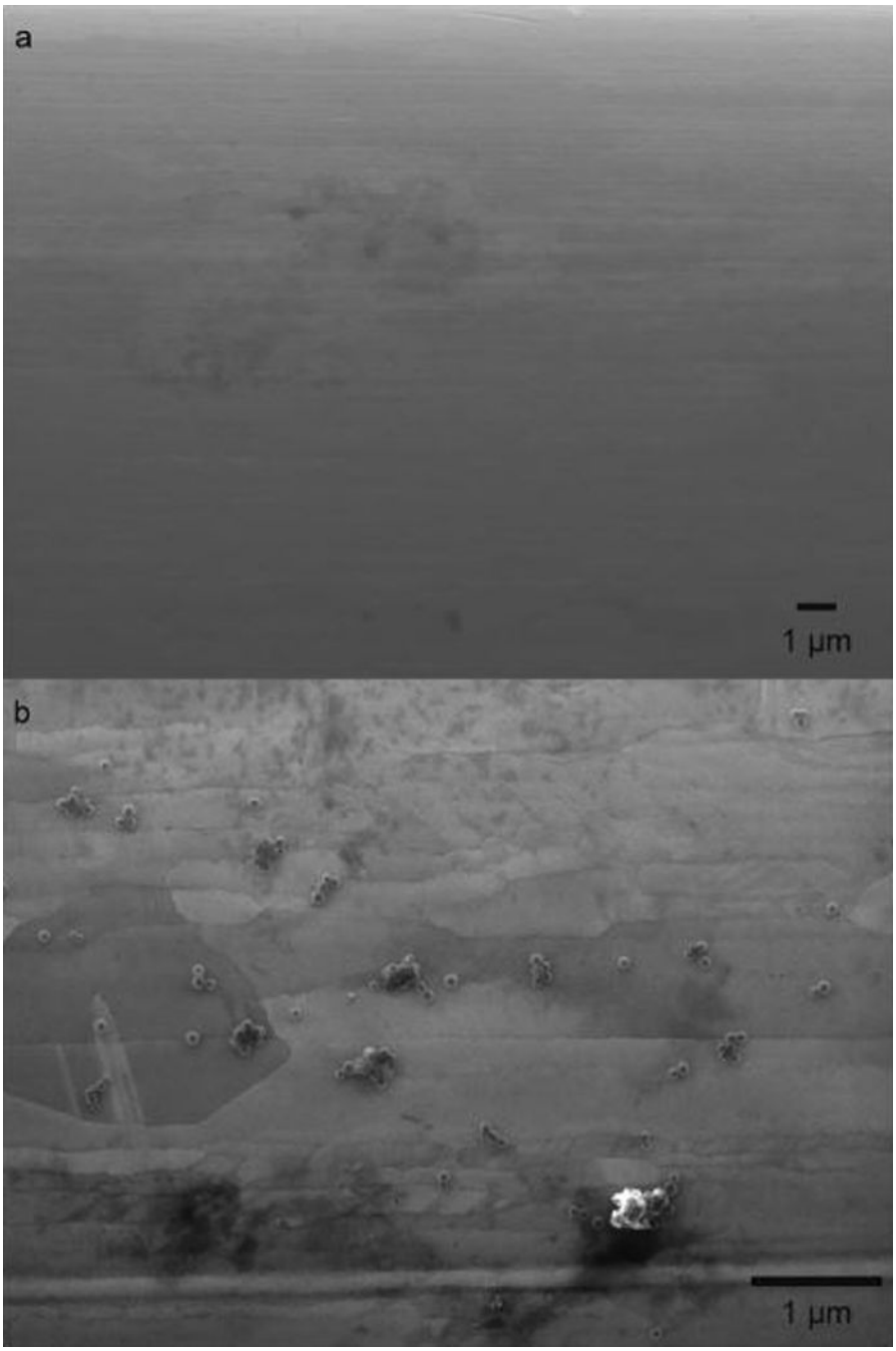

Figure 5.
SEM images a) before and b) after modification with 1×10^6 SA particles mL^{-1} (100 nm diameter) in a static-ePAD.

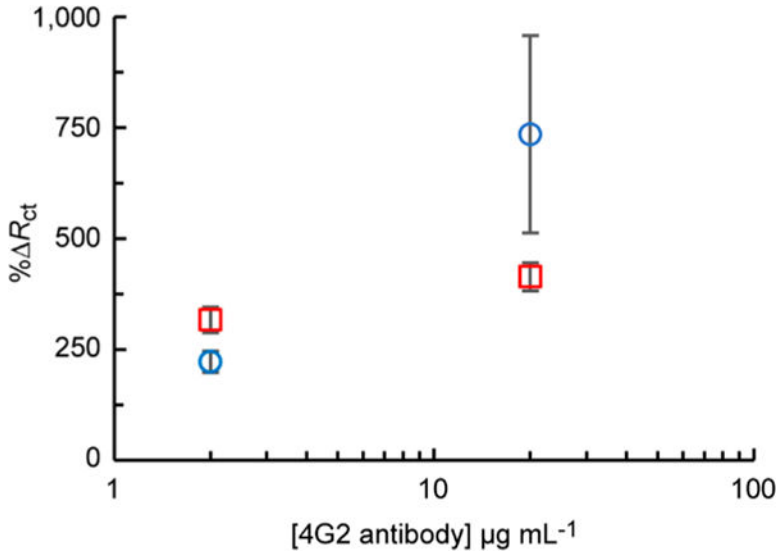

Figure 6.

Optimization of 4G2 antibody concentration for Au microwire modification. $\%\Delta R_{ct}$ measured for $[Fe(CN)_6]^{3/4-}$ impedance before and after addition of 1×10^6 WNV particles mL^{-1} (blue circles) or viral media (red squares) to flow-ePADs ($n = 4$).

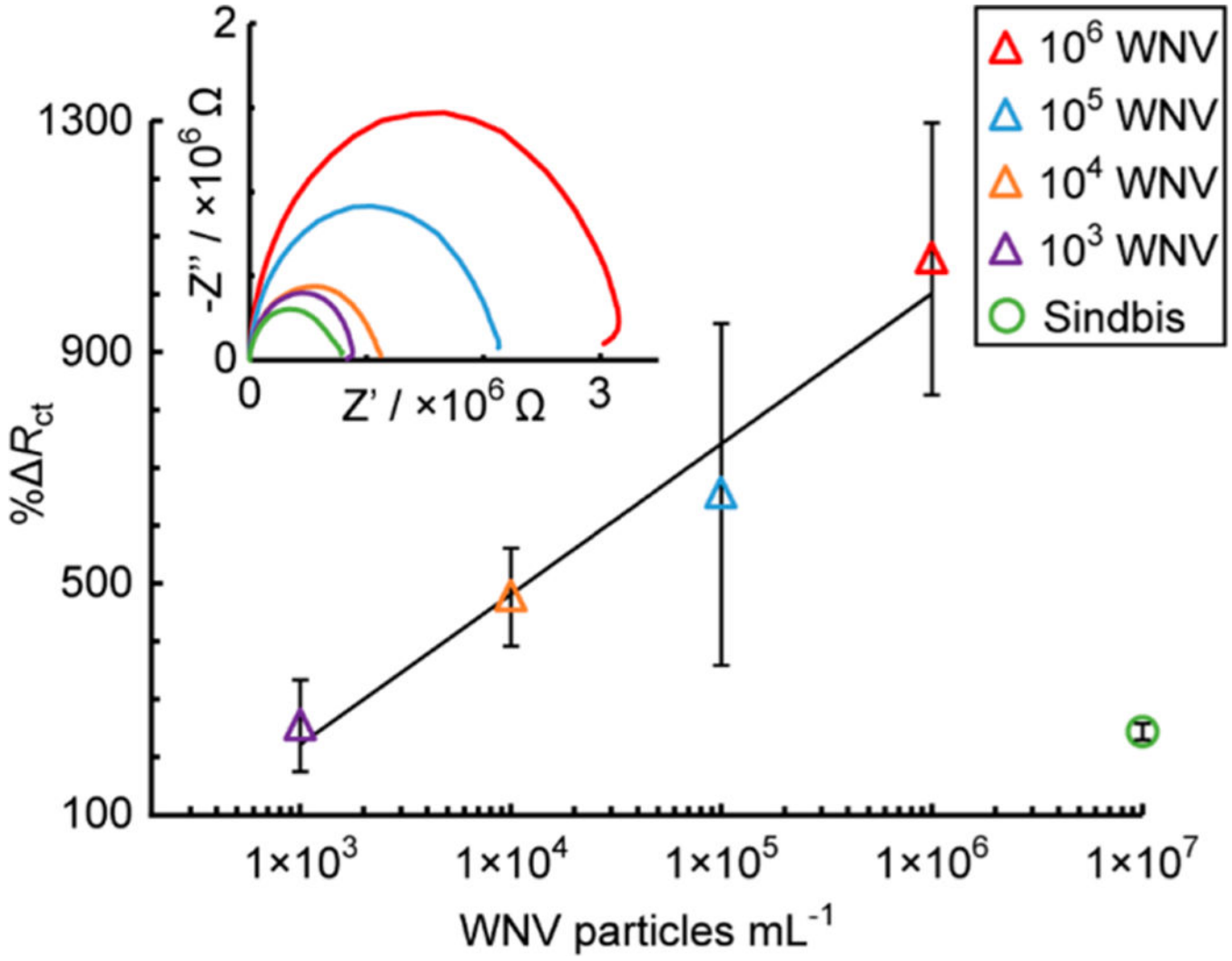

Figure 7.

Calibration curve (blue triangles) for different concentrations of WNV particles in a 50 μL aliquot of cell culture media (R^2 = 0.9650, n = 4) and a nonspecific test with Sindbis virus particles (red circle, n = 2) added to antibody-modified microwires in a flow-ePAD.